

Selected conducted electromagnetic interference issues in distributed power systems

R. SMOLEŃSKI*

University of Zielona Góra, Institute of Electrical Engineering, 50 Podgórna St., 65-246 Zielona Góra, Poland

Abstract. This paper addresses the specific issues associated with electromagnetic compatibility that should be taken into account at the developmental stage of distributed systems. The main aim is to establish how far conducted interferences can penetrate the electric grid and how the group of converters, which individually meet EMC standards, influence the mains supply. The measured results of the spread of electromagnetic interference (EMI) current over a typical local electric grid and the low and medium voltage side of the power transformer are presented. The commonly applied, in distributed power systems, four-quadrant converter has been used as a test interference source. The limitations in the applicability of standardized methods for evaluation of aggregated conducted interferences have been presented in a system consisting of a group of two-quadrant frequency converter drives.

Key words: electromagnetic compatibility, conducted interferences, distributed power systems, renewable energy systems, power converters.

1. Introduction

Currently, the four-quadrant frequency converter is often applied in various configurations of modern distributed systems of electric energy generation, transmission and conversion [1–4]. This converter typically generates a high level of electromagnetic interferences, especially in the conducted interference frequency range [5]. The high emission results from an energy conversion method utilizing two three-phase bridges which can adversely influence both line and load side. The analysis of electromagnetic compatibility of a four-quadrant converter and propositions for effective filtration methods have been presented in previous papers [6]. This paper presents a continuation of the research concerning penetration of the interferences deep into the electric grid. Additionally, interferences introduced into the mains by the group of two-quadrant frequency converters are evaluated. It has been shown that the standardized methods of the conducted EMI measurements are useless or give erroneous results for a system consisting of several converters, because of the phenomena accompanying the interference summation.

2. CM interferences generated by four-quadrant frequency converter

The origin of common mode (CM) interference is the CM voltage source, which inevitably exists in the system as the result of temporary electrical asymmetry at its neutral point. This asymmetry is caused by a pulse width modulation strategy using a three-phase two-level converter bridge. The common mode voltage in 3-phase circuits is defined as one third of the sum of phase voltages. CM currents emerge as a result

of transistor switching in the active rectifier and the inverter, due to a high du/dt value of the CM voltage [1, 5, 6].

Primary investigations showed minor influence of the load state and quadrant of operation on both the level and the shape of the CM current, therefore in all cases the drive was operated in the forward motoring quadrant under no-load condition. Additionally, the results of measurements in the frequency domain and analyses of the oscillatory modes revealed that in a four-quadrant AC drive system presented in Fig. 1 there are two CM voltage sources [6]; the first one on the line side of the converter and the second one on the motor side.

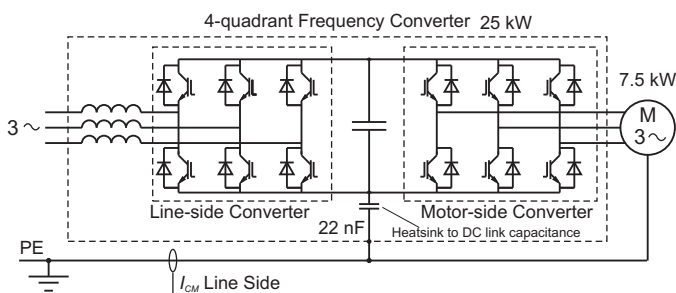


Fig. 1. Scheme of four-quadrant frequency converter drive

The CM current, measured using wideband current probe in PE wire on the line side of the converter for different time scales, is presented in Fig. 2.

The CM current on the line side of the converter has a damped oscillation shape of amplitude equal to 10 A and frequency of the main oscillatory mode approximately 70 kHz. The transistors switching instants (visible in Fig. 2 and Fig. 3) are synchronized by sample and hold (S&H) unit with fre-

*e-mail: R.Smolenski@ice.uz.zgora.pl

quency equal to 40 kHz. The RMS value of this current can exceed 1 A (1.2 A in Fig. 2).

The flow of CM current causes voltage drops on the common mode impedance of the electric grid, which are visible as high frequency disturbances of the same shape in each of the phase voltages (Fig. 3). The presented CM voltage on the supply terminals is equal to one third of the sum of the phase voltages.

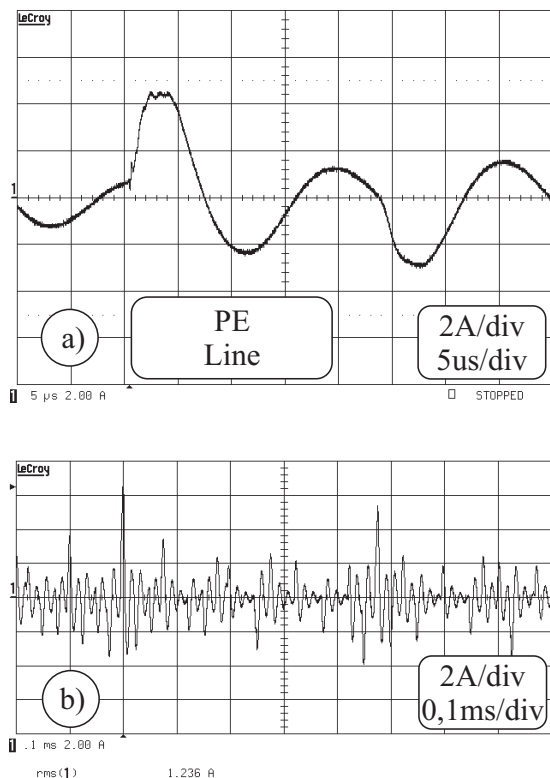


Fig. 2. CM current on the line side of the converter: (a) expanded form, (b) wide range time scale

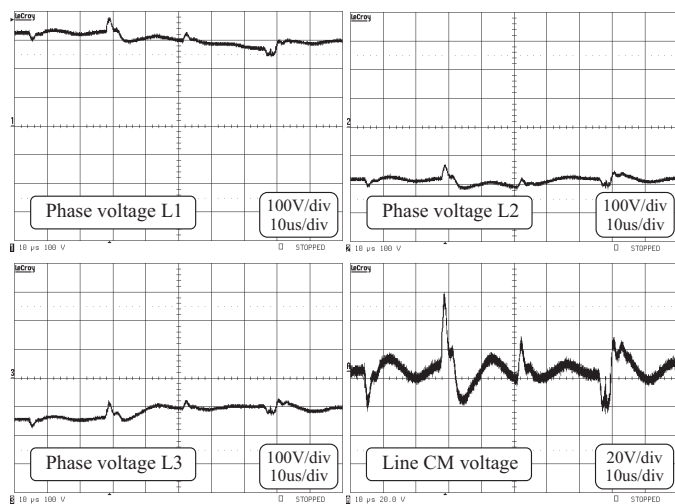


Fig. 3. Phase voltages and CM voltage at the input terminals of the converter

3. Flows of CM interferences generated by a four-quadrant frequency converter in a local electric grid

The main reason for presented investigations concerning the depth of interference penetration into mains is the high level of conducted interferences generated in 9 kHz–150 kHz (CISPR A) frequency band and the observed disturbances of electronic equipment. These operational abnormalities were caused by a converter located in remote circuits. In order to evaluate the depth of interference penetration into the electric grid the measurements of CM currents in PE wires at different points of a local main had to be performed. The converter was connected directly to the mains without LISN (Line Impedance Stabilization Network). The result of CM current measurement in CISPR A frequency band, using peak (upper line) and average (lower line) detectors, is shown in Fig. 4. The main frequency modes (S&H clock frequency 40 kHz, and envelope of spectra typical for damped oscillatory mode of 70 kHz) observed in the spectrum are related to those in the time domain presented in Fig. 2.

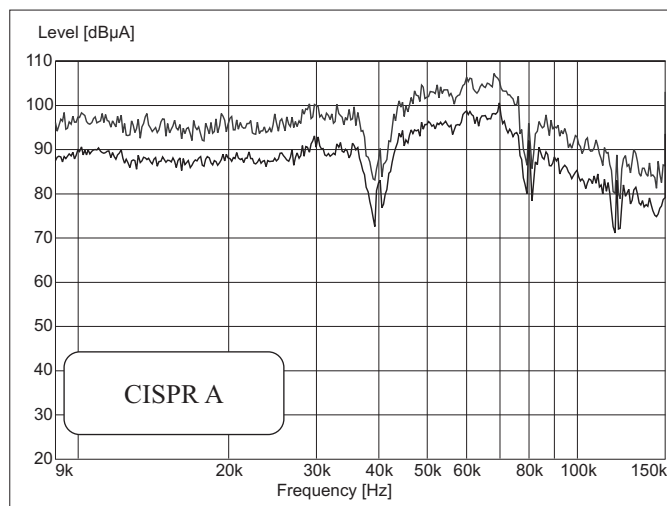


Fig. 4. Spectrum of CM current in converter PE wire

Figure 5 shows the spectrum of CM current measured using current probe in the PE wire of a power supply cable that supplies a laboratory. A measuring point was located at a transformer station near a common PE bus more than 200 m away from the interference source. Figure 5a shows the spectrum of background noise in cable PE wire and Fig. 5b shows the spectrum of CM current measured in the same point during a converter operation. The level of the CM interference increases significantly. At a frequency of 60 kHz, which constitutes the main oscillatory mode of the current, the level of interference increased 100 times (40 dB) compared to background interference. The observed level is only 20 dB lower in comparison with interference measured in the PE wire near the converter in spite of the existence of many alternative paths for the interference flow in the laboratory hall.

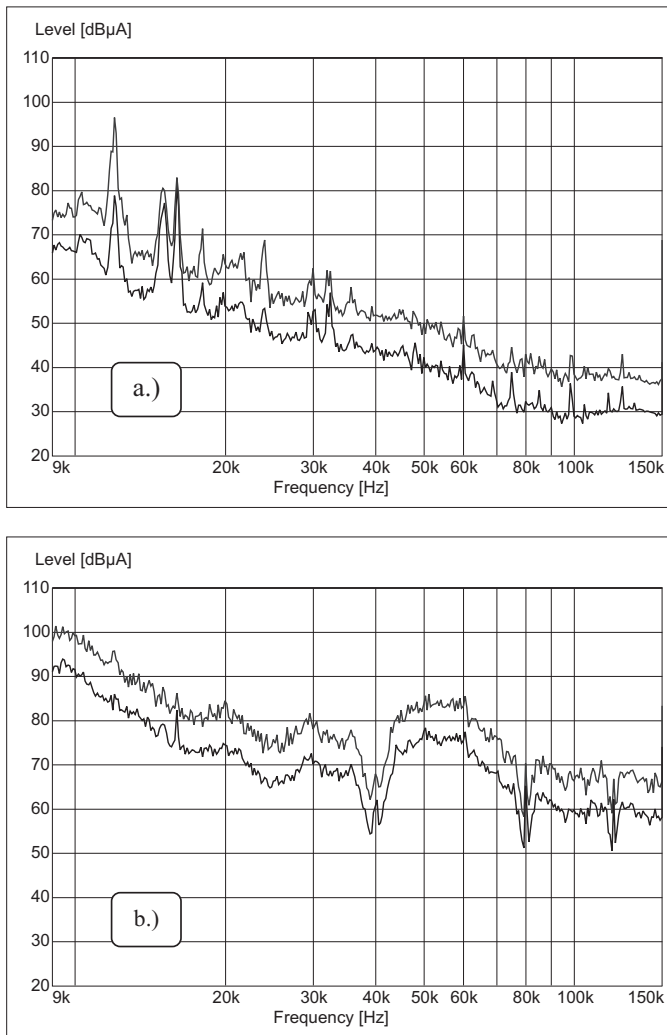


Fig. 5. Spectra of current in PE wire of power cable for: (a) converter switched off, (b) converter switched on

Figure 6 shows the results of investigations performed for part of the 150 kHz–30 MHz (CISPR B) frequency band (there was no significant interference above 5 MHz). The presented CM current spectra were measured in the PE wire near the converter (Fig. 6a) and in the PE wire of the power cable inside the transformer station for a switched on (Fig. 6b) and a switched off converter (Fig. 6c). Aside from initial part of the analyzed bandwidth, interference generated by the converter, measured by a peak detector, increased slightly compared to background noise. However, significant differences reached 20 dB and appeared in a CM current spectra measured using an average detector up to 2 MHz. The average detector level grows with increased rate of the appearance of the interference currents. Observed differences between peak and average detectors levels (Fig. 6b and Fig. 6c) mean that the CM currents in power cable PE wire of the highest amplitudes (peak detector levels) appears in the local low voltage grid even when the converter is switched off. However, the increased interference level measured using average detector, in a case of the switched on converter, shows that the rate of the appearance

of the CM currents of the highest amplitudes (peak detector) is much higher in the case of the operating converter.

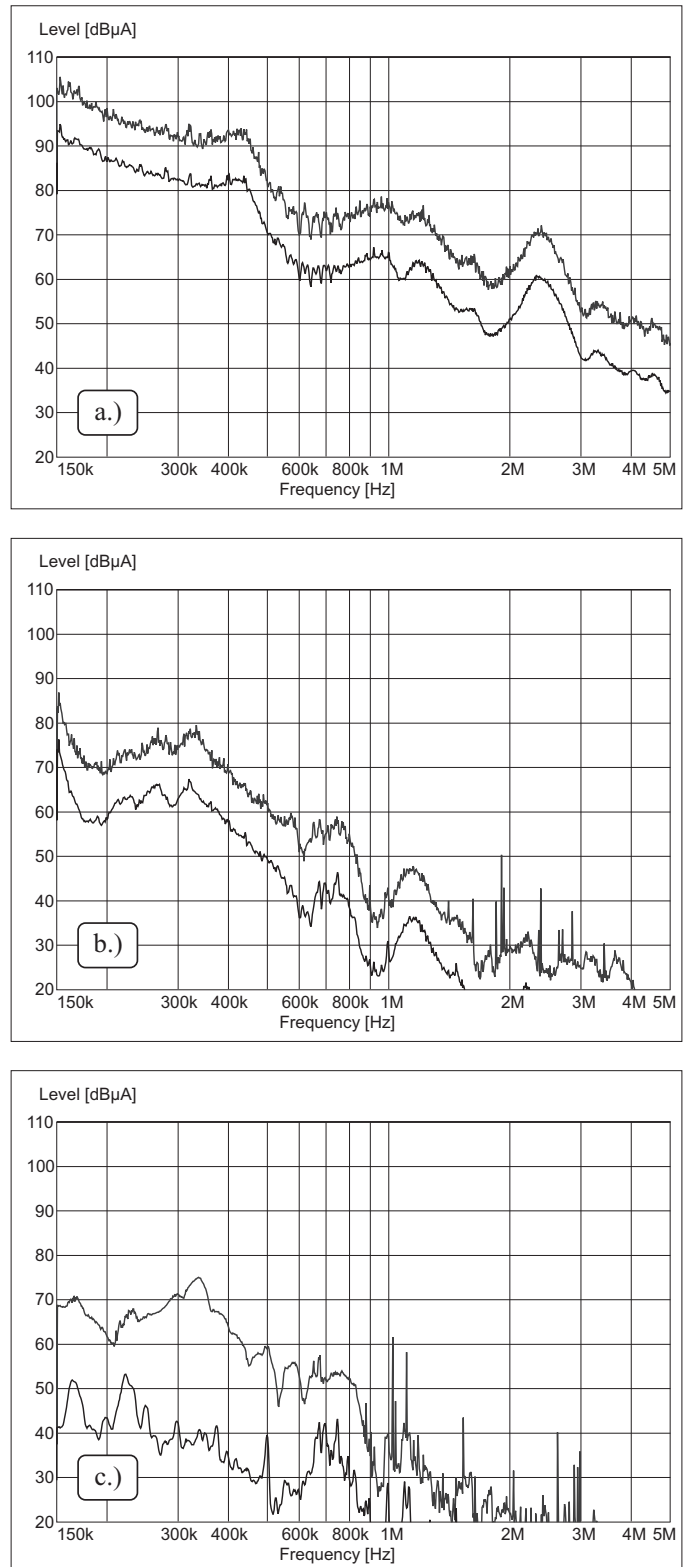


Fig. 6. Spectra of current in PE wire: (a) near converter, (b) in transformer station for switched on converter, (c) in transformer station for switched off converter

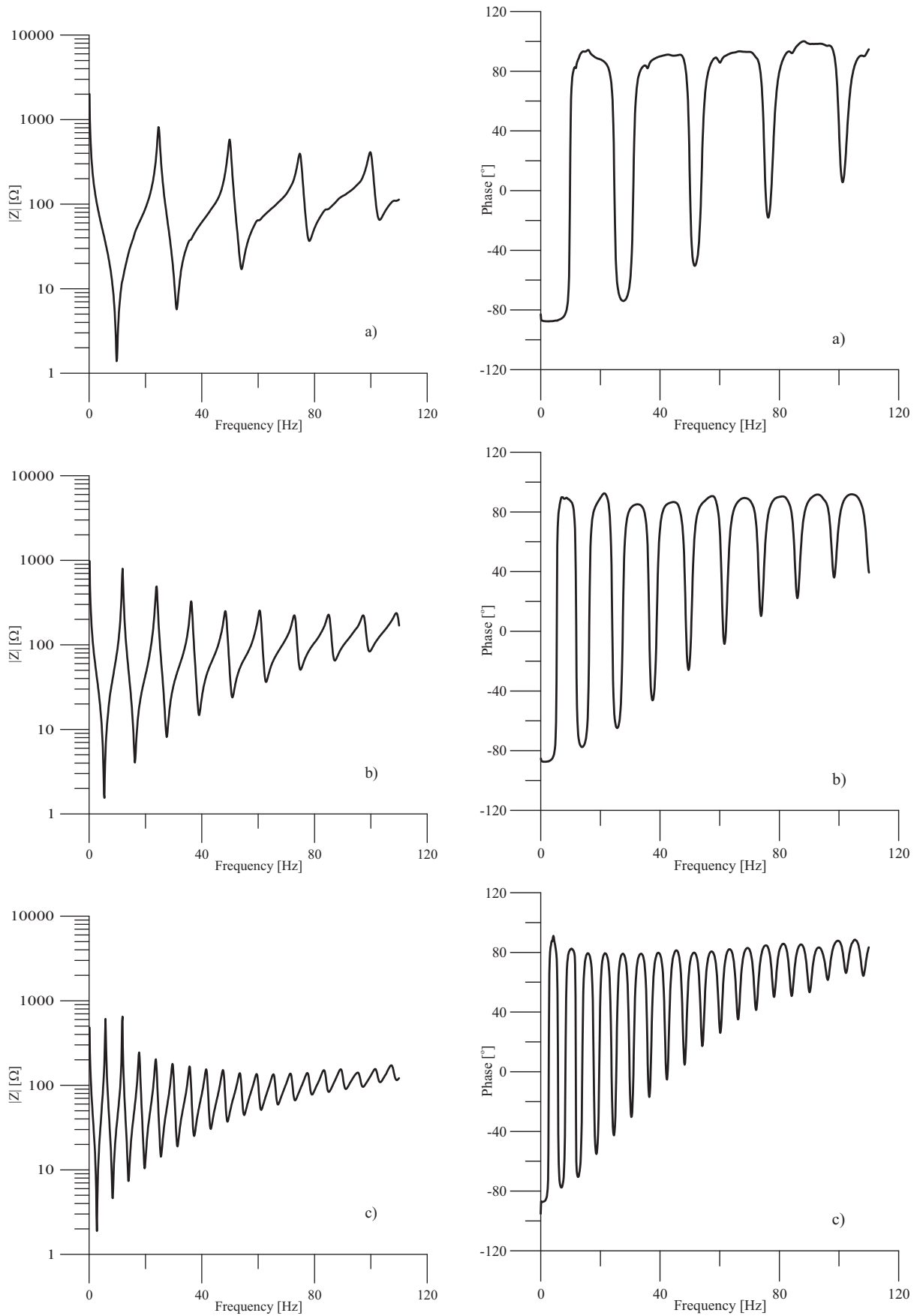


Fig. 7. CM impedance module and phase of YAKY $4 \times 25 \text{ mm}^2$ cable: (a) 2.5 m long, (b) 5 m long, (c) 10 m long

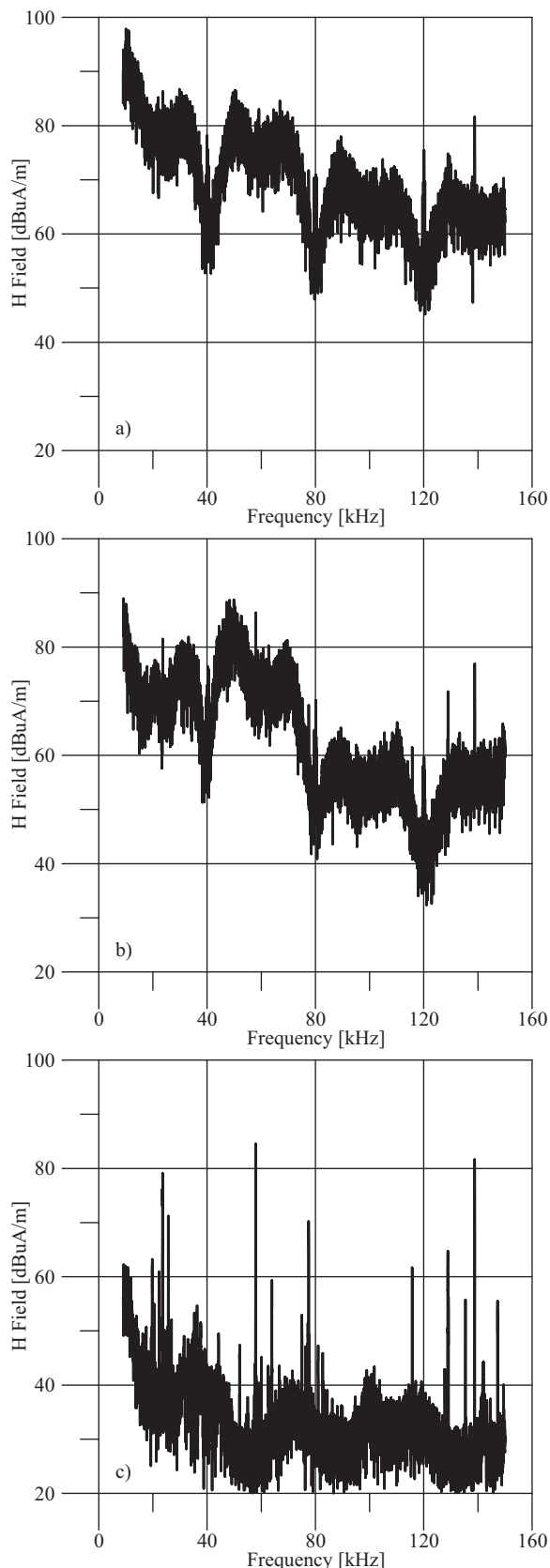


Fig. 8. Magnetic field: (a) on low voltage side of the transformer and switched on drive, (b) on medium voltage side of the transformer and switched on drive, (c) on medium voltage side of the transformer and switched off drive

Short rising and falling times of the heatsink to DC-link voltage which shape CM voltage and typical extensiveness of interference circuits mean that interference current paths have to be treated as distributed parameter circuits. A natural approach to the problem of interference spread analysis is to use the travelling wave approach [7, 8]. The usefulness of this method of analysis has been confirmed in papers concerning interference current paths in adjustable speed drives [9]. It is important to note that power cables typically work in a wave impedance mismatching condition. A mismatching of a cable wave impedances causes multiple reflections and interferences that along with a nonlinear cable frequency characteristics modify shape and resonant oscillation modes in CM currents. Those phenomena make difficult an identification of the sources of the interference currents measured in different points of the distributed systems. Please note the differences in the main oscillatory modes of the CM currents generated by 4-quadrant drive in the different points of the local grid e.g.: 70 kHz in Fig. 4 and 60 kHz in Fig. 5b. Figure 7 shows the module and phase of CM impedance for different lengths of YAKY $4 \times 25 \text{ mm}^2$ power cable. The presented results show that high frequency interferences in the megahertz range are relatively strongly damped. The module and phase of CM impedance in CISPR A frequency range significantly depends on cable length, type and interference frequencies. The two-terminal CM impedance measurements have been confirmed by analysis of the cable insertion loss.

Further analyses were carried out in a low/medium voltage power transformer station. The four-quadrant drive was fed by a 3 m long cable from the low voltage side of the transformer. Figure 8 shows CM current in the cable PE wire, with magnetic field measured by loop antenna on the low and medium side of the transformer. It is important to note that the low and the medium side of the transformer in question were located on different sides of the building.

We can observe a typical shape of the spectra generated by the converter on both low and medium sides of the transformer station. Because of capacitive couplings in the high frequency range the interference patterns are not transformed according to transformer voltage ratio. However, significant capacitive couplings mean that interference on the medium voltage side reach a high level as well.

4. Conducted EMI generated by two-quadrant converter drives

The two quadrant frequency converter drives are increasingly being used in modern industrial systems. The increasing number of the converters might cause the immunity problems of the electronic equipment in nearby system because of summed interferences. The problems linked with the adverse influence of the group of power electronic converters on electric grid have been presented on the basis of the system consist of three almost identical two-quadrant converter drives.

The CM currents, which are generated by switching states of the single inverter [10–14], have an impulse-like waveform with HF oscillation. The resonant frequency of the oscillatory

mode is determined by the residual, parasitic parameters of the CM current path (Fig. 9). The CM currents split according to the proportion of the divider created by HF impedance in the inverter grounding point. The main return path for the CM currents leads through the heat sink to DC link capacitance [9].

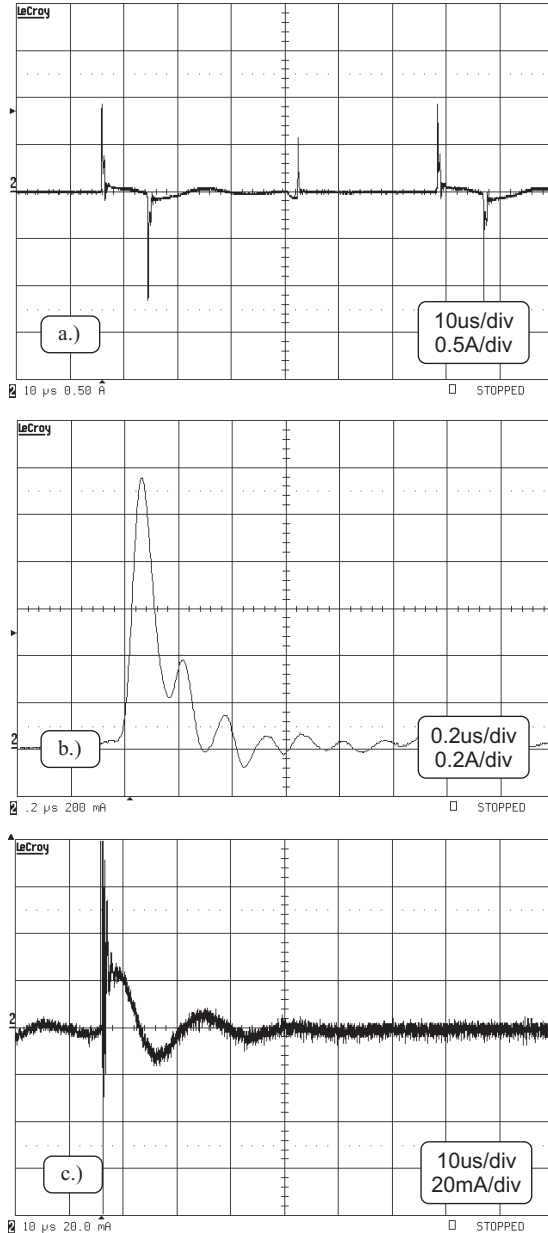


Fig. 9. (a) Common mode current in motor PE wire, (b) HF component of CM current, (c) LF oscillatory of CM current

The CM current causes a CM voltage drop in the heatsink to DC link capacitance. In a blocking state of the rectifier diodes, only the higher frequency part (oscillatory modes of approximately 160 kHz and 6.8 MHz) of this current flows through the series parasitic capacitance of the diode and converter supply arrangement, Fig. 10c. In the conduction state, the voltage drop in the heatsink to DC link capacitance causes oscillation of the relatively low frequency (approximately

16 kHz) in the shape of CM current that flows in closed loop consisting of a DC-link-to-heatsink capacitance, the resultant inductance of the mains (or LISN), the cable and the input filter, Fig. 10b. The CM current (i_{CM}) and phase current (i_p) on the line side of the converter in conduction and blocking states of the rectifier diodes are shown in Fig. 10.

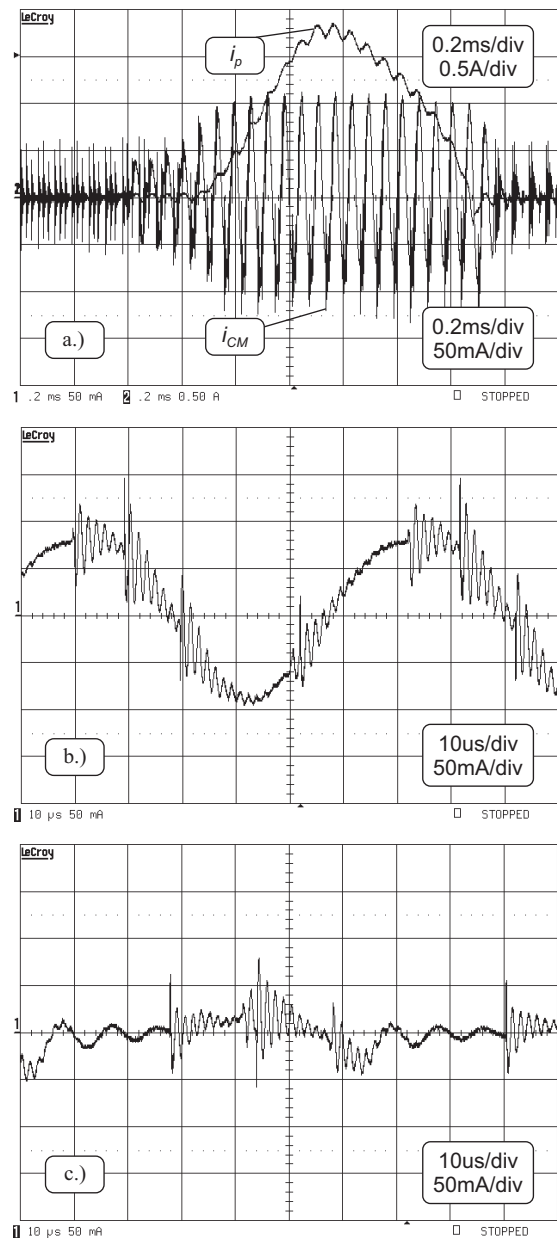


Fig. 10. (a) CM current on the line side of the converter and rectifier phase current, (b) CM current in conduction state of the rectifier, (c) CM current in blocking state of the rectifier

The time of appearance of both CM and differential mode (DM) currents depends on the switching instants resulting from the inverter control algorithm. Additionally, the current level and the oscillation frequency are modulated by the conduction state of the input rectifier. Figure 11 shows the spectrum of the CM current on the line side of the converter

measured using spectrum analyzer with resolution bandwidth equal to 10 Hz. There are sideband harmonics equal to 300 Hz resulting from the use of a 6-pulse rectifier that modulates amplitude of the inverter carrier frequency as it was earlier presented in the time domain, Fig. 10a. This phenomenon is only slightly visible in normalized EMI measurements because of the selectivity of the intermediate frequency bandwidth of the EMI receivers that is equal to 200 Hz for CISPR A frequency band. The obtained results of investigations were confirmed in the system comprising frequency converter drive with the single-phase input rectifier.

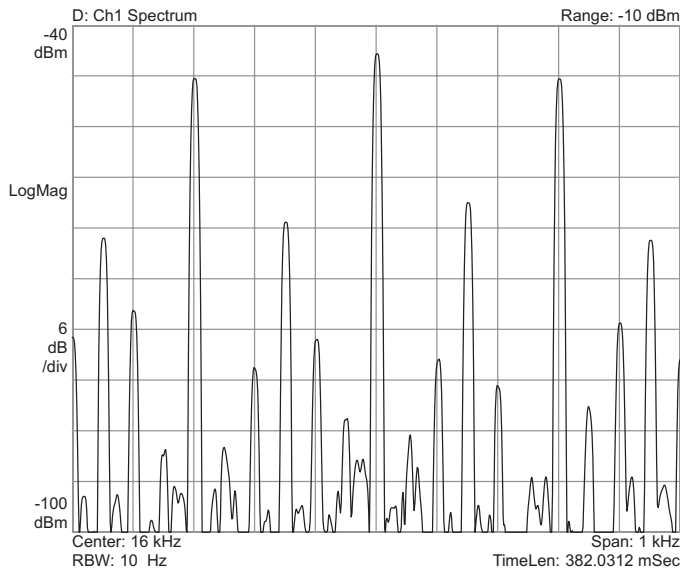


Fig. 11. Spectrum of line side CM current at carrier frequency with sideband harmonics caused by 6-pulse rectifier

5. Aggregated conducted interferences generated by a group of two-quadrant frequency converter-fed drives

The European Community Directive 2004/108/EC states: “Where apparatus is capable of taking different configurations, the electromagnetic compatibility assessment should confirm whether the apparatus meets the protection requirements in the configurations foreseeable by the manufacturer as representative of normal use in the intended applications; in such cases it should be sufficient to perform an assessment on the basis of the configuration most likely to cause maximum disturbance (...)”. This means that producers of power electronic converters for distributed power systems should take into account the influence of aggregated interferences introduced to the power grid by the group of converters rather than electromagnetic emission of the single item of the equipment.

Investigations that show measuring difficulties in such multi-converter systems were carried out in a system consisting of three identical 1 kW induction motor drives (drive 1, drive 2 and drive 3) fed by 7.5 kW frequency converters supplied via LISN. The scheme of the frequency converter with EMI filter comprising CM choke and capacitors (X and Y class) is presented in Fig. 12.

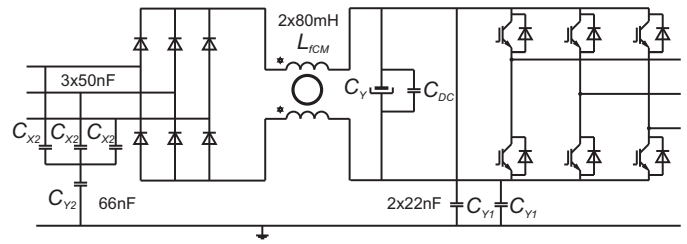


Fig. 12. Frequency converter scheme with EMI filter arrangement

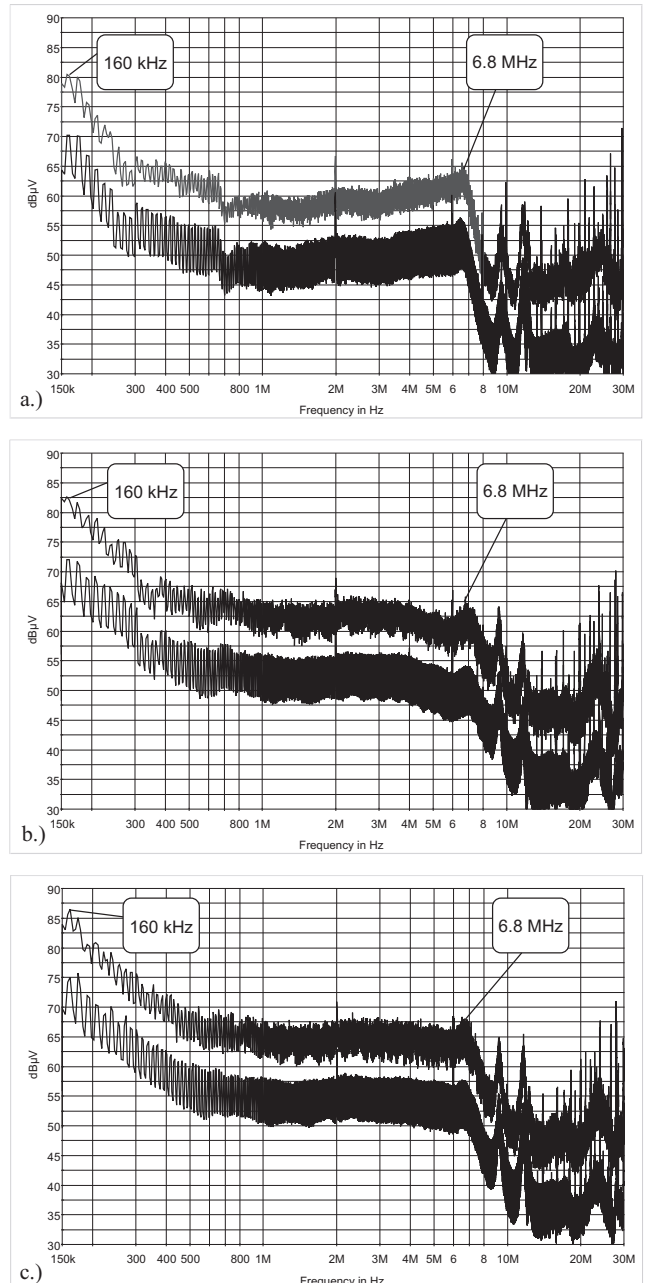


Fig. 13. Conducted EMI spectra (peak and average detectors) according to EN 61800-3: (a) drive 1 operated, (b) drives 1 and 2 operated, (c) drives 1, 2 and 3 operated

The measured results in system of Fig. 12 are presented in Fig. 13. In order to ensure unchangeable interference current circuits all of the frequency converters were connected to

LISN for the whole measurement period. Only inverters were switched on/off. The measurements for single drive, two and three drives were carried out as if for one piece of equipment in full compliance with EN 61800-3.

All of the oscillatory modes can be distinguished as those presented in a time domain current waveform (Figs. 10 and 11) [15, 16]. It is possible to observe that conducted EMI introduced into the electric grid by a group of the converter drives can be much higher than the level of EMI generated by a single drive. This means that we might expect an increased number of EMC related problems in systems containing a large number of converters. In order to establish how interferences are aggregated additional tests not required by standards are performed.

Figure 14 shows an additional test for CISPR A frequency band IF BW = 200 Hz.

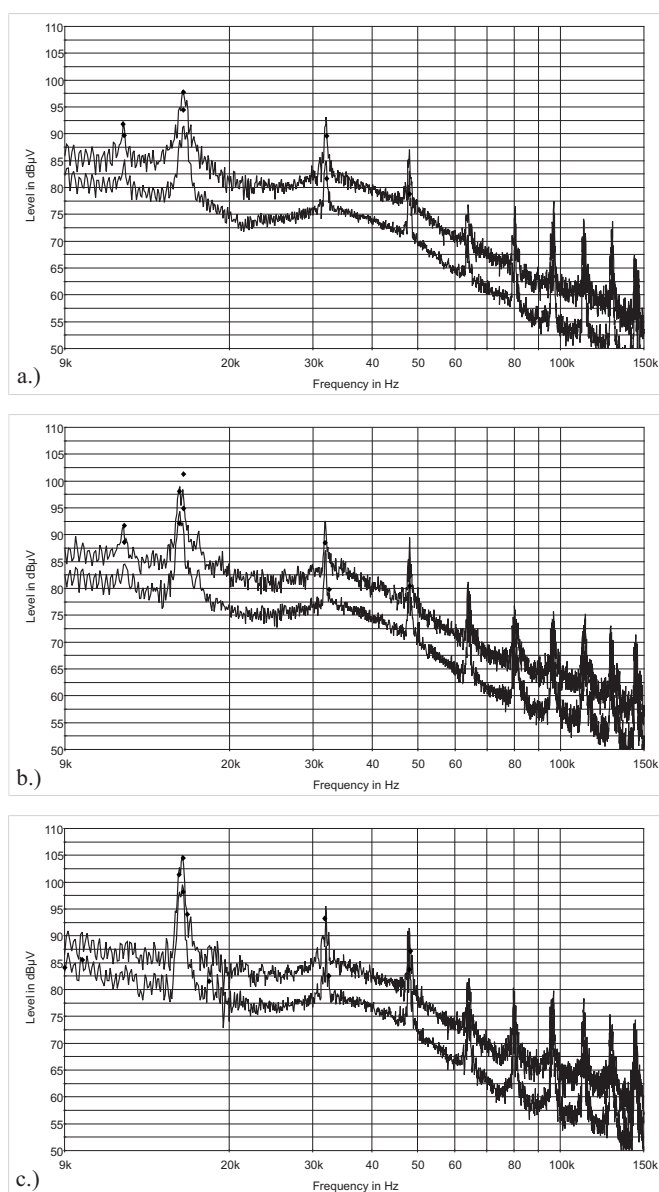


Fig. 14. Conducted EMI spectra according to CISPR A range: (a) drive 1 operated, (b) drives 1 and 2 operated, (c) drives 1, 2 and 3 operated

In CISPR A frequency band the level of measured interference patterns increases with a rising number of operating converters as well. The level differences between single drive and triple drives reached 8dB. However, quasi-peak detector levels higher than peak detector levels (point in Fig. 14b) and differences in results obtained for double and triple drives, in multiple tests with the same measuring conditions indicated that signals had been modulated by a very slowly changeable envelope.

The spectrograms presented in Fig. 15 show a CM current level variation of 16 kHz harmonic with sidebands vs. time for a) drive 1, b) drives 1 and 2, c) drives 1, 2 and 3. The spectrograms illustrate the changes in the level of carrier harmonic, presented in Fig. 11, during 31.79 s. The bigger the number of operated converters, the higher the maximum level of the measured current was. However, the modulation envelope causes a decrease of the interference level below those measured in the case of a single drive.

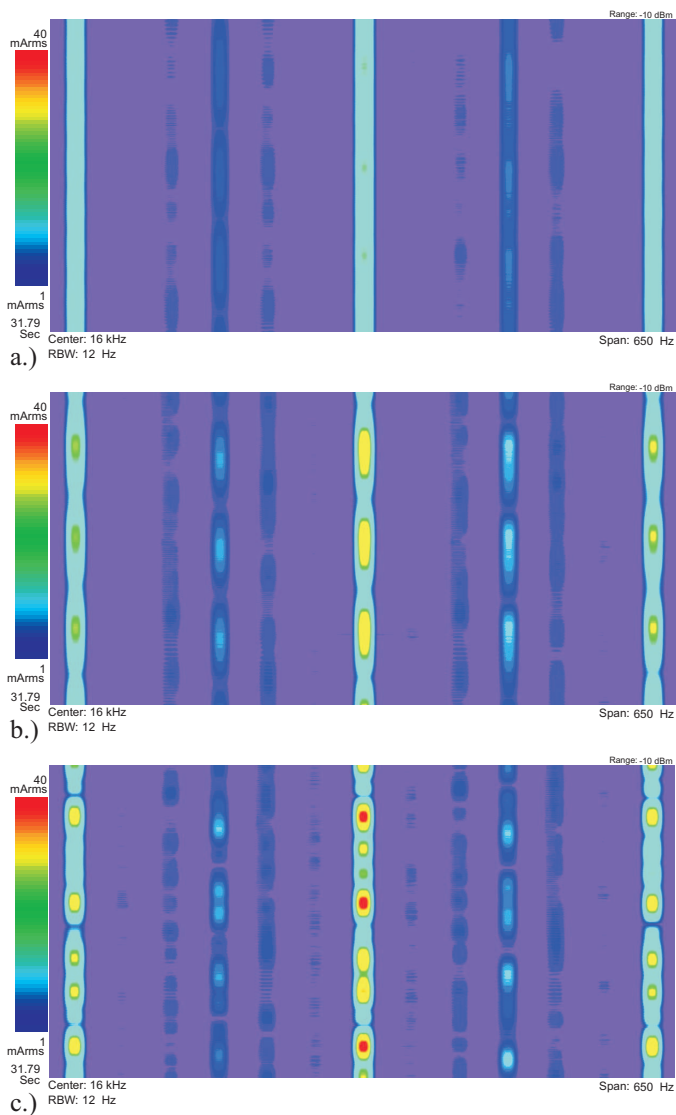


Fig. 15. Spectrograms of interference currents at carrier frequency for: (a) drive 1, (b) drives 1 and 2, (c) drives 1, 2 and 3 (colour on-line)

Selected conducted electromagnetic interference issues in distributed power systems

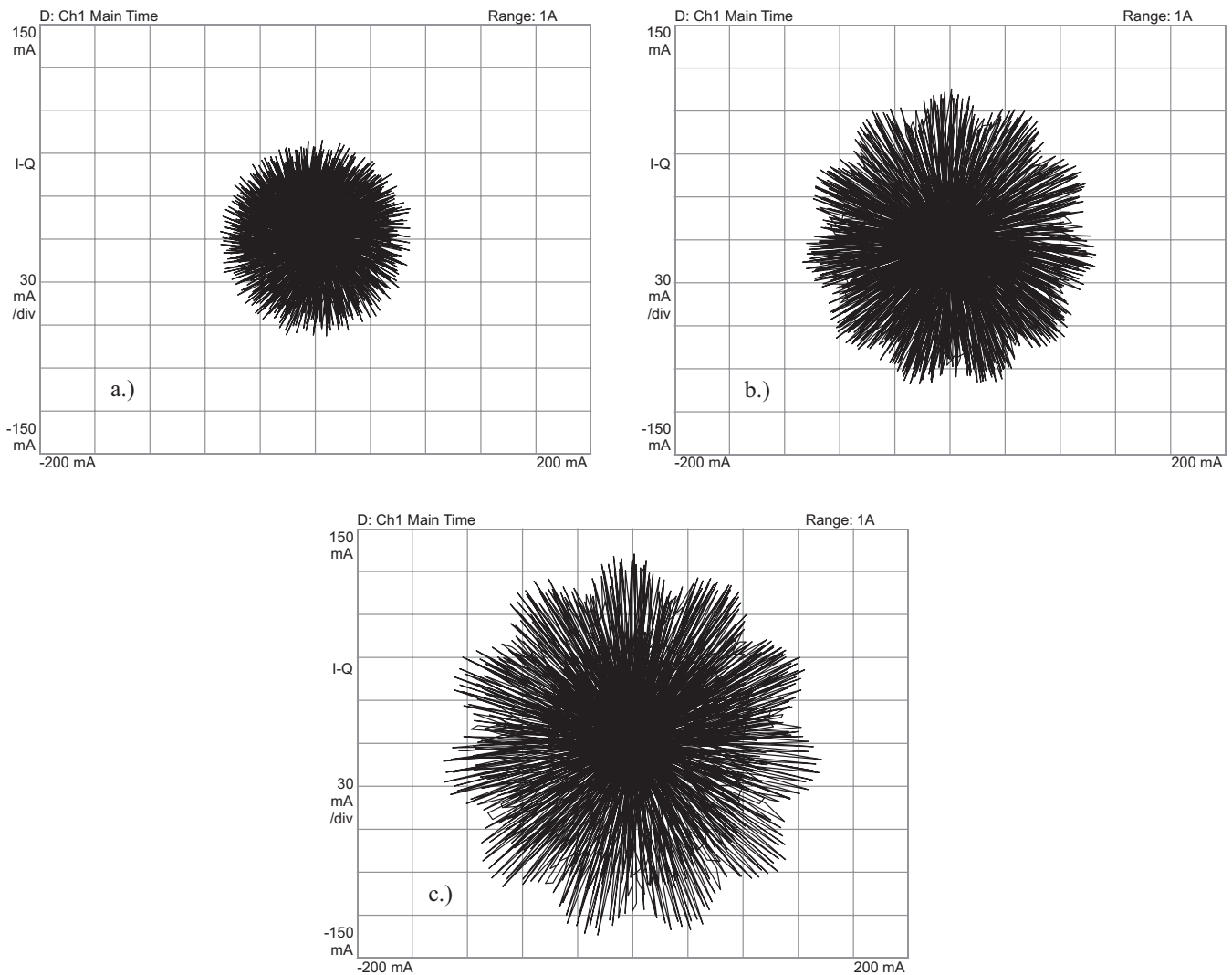


Fig. 16. Vector diagrams of maximum CM interference current levels for: (a) drive 1, (b) drives 1 and 2, (c) drives 1, 2 and 3

It is important to note that semiconductors act just like the RF detector in a crystal radio set and will demodulate any RF signals [17]. Immunity measurement practice has shown that electronic equipment is much more sensitive to modulated signals. In systems consisting of many converters controlled using different algorithms we should expect wideband envelopes of interference patterns that may cause many problems in ensuring equipment immunity.

The vector signal analysis is a useful method that can be successfully applied to the investigation of modulation influence on interference.

Figure 16 shows a vector diagram of the maximum levels of the sum of the CM currents for: (a) single drive, (b) two drives, (c) three drives. The raising of current level and its modulation effects are easy to evaluate.

The histograms presented in Fig. 17 show the distributions of thousand final measurements taken according to require-

ments of the EMC standards. Measurements were carried out using average detector for 16 kHz and typical final measuring time equal to 1 second for switching frequency.

The dispersion of average detector levels for two and three drives those operated simultaneously is caused by low frequency envelopes that modulate the interference levels. The significant differences reached 17 dB (eight times) showed ineffectiveness of standard measuring procedures for the evaluation of the aggregated conducted interferences generated by the group of converters. The highest level recorded for three drives operated together was 6 dB bigger than the highest level observed for the drive 2 in a case of the single drive operation. This means that EMC assurance of the single power electronic converter might be insufficient to fulfill EMC Directive requirements concerning multi-converter power systems.

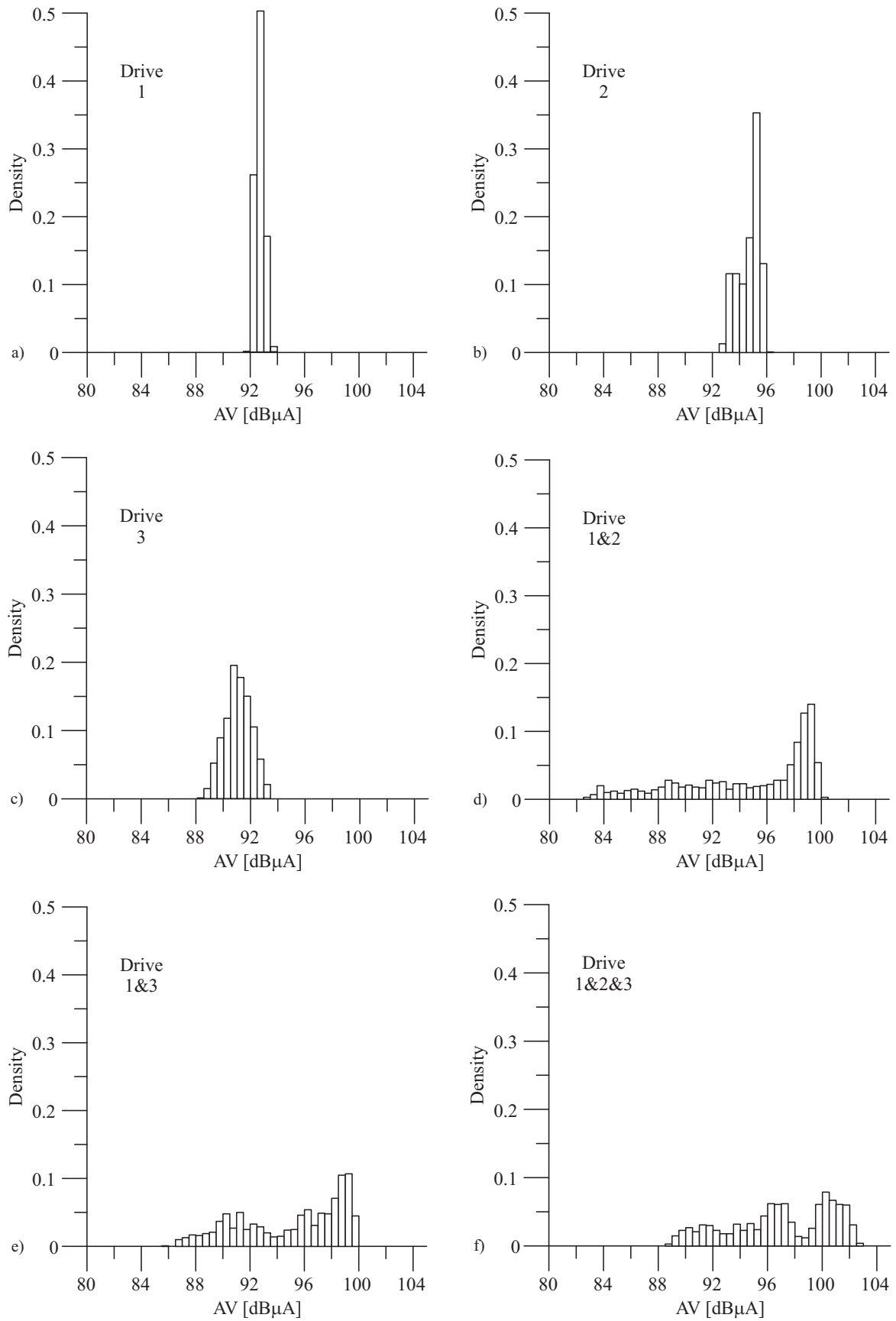


Fig. 17. Histograms of average detector levels for switched on: (a) drive 1, (b) drive 2, (c) drive 3, (d) drives 1 and 2, (e) drives 2 and 3, (f) drives 1, 2 and 3

6. Conclusions

The assurance of electromagnetic compatibility is an important factor conditioning the development of modern distributed power systems. The connection of susceptible control and communications electronic equipment to a high emission power electronics sector of a distributed system requires a special caution and in-depth EMC analysis to ensure system reliability.

The presented measurements have shown that interference caused by a four quadrant converter, which is often used in distributed power systems, can reach a distant point of the local low voltage grid. Interference coupled by common impedance might cause immunity problems in the distorted mains. Additionally, magnetic field measurements have shown that such interference can be transferred by parasitic couplings on the medium voltage side of the transformer.

The experimental results have also shown that the aggregated interference components introduced into the electric grid by the system and consisting of the same power electronic converters that individually fulfill EMC requirements might act as an incompatible unit. These kinds of systems may cause problems with both internal and external electromagnetic compatibility.

It can be observed that aggregated interference signals are modulated by slowly changeable envelopes that cause measuring difficulties. Normalized tests with their typical measuring times are not sensitive enough to properly evaluate interference levels. In order to investigate the aggregated interference components in systems containing a group of power electronic converters some special measuring methods need to be developed.

Acknowledgements. Scientific work financed from the scientific research resources in years 2009–2011 as the research project no. N N510 333537.

REFERENCES

- [1] G. Benysek, *Improvement in the Quality of Delivery of Electrical Energy Using Power Electronics Systems*, Springer-Verlag, London, 2007.
- [2] N. Hingorani and L. Gyugyi, *Understanding FACTS: Concepts and Technology of Flexible AC Transmission Systems*, Wiley-IEEE Press, New York, 2000.
- [3] Y. Han, M. Khan, L. Xu, G. Yao, L. Zhou, and C. Chen, "A new scheme for power factor correction and active filtering for six-pulse converters loads", *Bull. Pol. Ac.: Tech.* 57 (2), 157–169 (2009).
- [4] Z. Chen, X. Zhang, and J. Pan, "An integrated inverter for a single-phase single-stage grid-connected PV system based on Z-source", *Bull. Pol. Ac.: Tech.* 55 (3), 263–272 (2007).
- [5] A. Kempski, R. Smoleński, and R. Strzelecki, "Conducted EMI in four-quadrant AC drive system", *Proc. EPE-PEMC 2*, 31–36 (2002).
- [6] A. Kempski, R. Strzelecki, R. Smoleński, and G. Benysek, "Suppression of conducted EMI in four-quadrant AC drive system", *Proc. IEEE-PESC'03* 3, 1121–1126 (2003).
- [7] P.C. Magnusson, G.C. Alexander, V.K. Tripathi, and A. Weishaar, *Transmission Lines and Wave Propagation*, CRC Press, Boca Raton, 2001.
- [8] G. Skibinski, R. Kerkman, D. Leggate, J. Pankau, and D. Schlegel, "Reflected wave modelling techniques for PWM AC motor drives", *Proc. APEC 2*, 1021–1029 (1998).
- [9] A. Kempski, R. Smoleński, and R. Strzelecki, "Common mode current paths and their modelling in PWM inverter-fed drives", *Proc. IEEE-PESC'02* 3, 1551–1556 (2002).
- [10] H. Akagi and T. Doumoto, "A passive EMI filter for preventing high-frequency leakage current from flowing through the grounded inverter heat sink of an adjustable-speed motor drive system", *IEEE Trans. on Ind. Appl.* 41, 1215–1223 (2005).
- [11] H. Akagi, H. Hasegawa, and T. Doumoto, "Design and performance of a passive EMI filter for use with voltage source PWM inverter having sinusoidal output voltage and zero common-mode voltage", *IEEE Trans. on Power Electronics* 19, 1069–1076 (2004).
- [12] H. Akagi and S. Tamura, "A passive EMI filter for eliminating both bearing current and ground leakage current from an inverter-driven motor power electronics", *IEEE Trans. on Power Electronics* 21, 1459–1469 (2006).
- [13] S. Ogasawara and H. Akagi, "Modelling and damping of high-frequency leakage currents in PWM inverter-fed AC motor drive systems", *IEEE Trans. on Ind. Appl.* 32, 1105–1113 (1996).
- [14] N. Hanigovszki, J. Poulsen, G. Spiazzi, and F. Blaabjerg, "An EMC evaluation of the use of unshielded motor cables in AC adjustable speed drive applications", *IEEE Trans. on Power Electronics* 21, 273–281 (2006).
- [15] J. Hu, J. van Bloch, and W. De Doncker, "Typical impulses in power electronics and their EMI characteristics", *Proc. IEEE-PESC'04* 4, 3021–3027 (2004).
- [16] G. Grandi, D. Casadei, and U. Reggiani, "Common- and differential-mode HF current components in AC motors supplied by voltage source inverters", *IEEE Trans. on Power Electronics* 19, 16–24 (2004).
- [17] T. Williams, K. Armstrong, *EMC for Systems and Installations*, Butterworth-Heinemann Ltd, Oxford, 2000.